Spectroscopic Evidence for Changes in the Redox State of the Nitrogenase P-Cluster during Turnover†

Jeannine M. Chan,‡ Jason Christiansen,§ Dennis R. Dean,*,§ and Lance C. Seefeldt*,‡

Department of Chemistry and Biochemistry, Utah State University, Logan, Utah 84322, and Department of Biochemistry−Fralin Biotechnology Center, Virginia Tech, Blacksburg, Virginia 24061

Received December 4, 1998; Revised Manuscript Received March 9, 1999

ABSTRACT: Biological nitrogen fixation catalyzed by nitrogenase requires the participation of two component proteins called the Fe protein and the MoFe protein. Each $\alpha\beta$ catalytic unit of the MoFe protein contains an [8Fe-7S] cluster and a [7Fe-9S-Mo-homocitrate] cluster, respectively designated the P-cluster and FeMo-cofactor. FeMo-cofactor is known to provide the site of substrate reduction whereas the P-cluster has been suggested to function in nitrogenase catalysis by providing an intermediate electron-transfer site. In the present work, evidence is presented for redox changes of the P-cluster during the nitrogenase catalytic cycle from examination of an altered MoFe protein that has the β-subunit serine-188 residue substituted by cysteine. This residue was targeted for substitution because it provides a reversible redox-dependent ligand to one of the P-cluster Fe atoms. The altered β-188^{Cys} MoFe protein was found to reduce protons, acetylene, and nitrogen at rates approximately 30% of that supported by the wild-type MoFe protein. In the dithionite-reduced state, the β-188^{Cys} MoFe protein exhibited unusual electron paramagnetic resonance (EPR) signals arising from a mixed spin state system ($S = {}^5/_2, {}^1/_2$) that integrated to 0.6 spin/$\alpha\beta$-unit. These EPR signals were assigned to the P-cluster because they were also present in an apo-form of the β-188^{Cys} MoFe protein that does not contain FeMo-cofactor. Mediated voltammetry was used to show that the intensity of the EPR signals was maximal near −475 mV at pH 8.0 and that the P-cluster could be reversibly oxidized or reduced with concomitant loss in intensity of the EPR signals. A midpoint potential (E_m) of −390 mV was approximated for the oxidized/resting state couple at pH 8.0, which was observed to be pH dependent. Finally, the EPR signals exhibited by the β-188^{Cys} MoFe protein greatly diminished in intensity under nitrogenase turnover conditions and reappeared to the original intensity when the MoFe protein returned to the resting state.

Biological nitrogen fixation is catalyzed by the nitrogenase complex, which is composed of two component proteins called the MoFe protein and the Fe protein (*1*). The MoFe protein is a 240 kDa $\alpha_2\beta_2$ tetramer that contains two pairs of metalloclusters. One of these, the FeMo-cofactor,[1] provides the site of substrate reduction, and the other, an [8Fe-7S] cluster (called the P-cluster), is thought to provide an intermediate electron-transfer site (*2*, *3*). The Fe protein is a 64 kDa homodimer that has one nucleotide-binding site on each subunit and a single [4Fe-4S] cluster bridged between the two subunits (*4*). During catalysis, the Fe protein donates one electron to the MoFe protein in a process that requires MgATP hydrolysis. Following electron transfer, the two component proteins dissociate in what is thought to be the overall reaction rate-limiting step (*5*). This process is repeated until sufficient electrons have accumulated within the MoFe protein for substrate reduction to occur.

A major challenge in nitrogenase research is to understand how the multiple electrons required for substrate reduction are accumulated within the MoFe protein. The P-cluster has been implicated as participating in this process (*6*−*8*), possibly by accumulating electrons delivered by the Fe protein prior to their delivery to the substrate reduction site (*9*). Indirect evidence supporting such a role for the P-cluster comes from several observations. First, the X-ray crystal structures of two different Fe protein−MoFe protein complexes both place the P-cluster between the Fe protein [4Fe-4S] cluster and the FeMo-cofactor (*10*, *11*). Second, a catalytically inactive form of the MoFe protein that contains an FeMo-cofactor derivative is still able to accept an electron from the Fe protein, revealing a new EPR signal that was attributed to the P-cluster (*6*). Third, an altered MoFe protein that has a substitution for an amino acid residue located between the P-cluster and the FeMo-cofactor has altered kinetic features that were attributed to a lower rate of electron transfer from the P-cluster to the FeMo-cofactor (*7*). Finally,

† Research supported by National Science Foundation Grants MCB-9722937 (to L.C.S.) and MCB-9630127 (to D.R.D.), USDA Postdoctoral Fellowship USDA-9603167 (to J.C.), and a Willard L. Eccles Foundation Fellowship (to J.M.C.).

* To whom correspondence should be addressed. L.C.S.: phone (435) 797-3964, fax (435) 797-3390, email seefeldt@cc.usu.edu. D.R.D.: phone (540) 231-5895, fax (540) 231-7126, email deandr@vt.edu.

‡ Utah State University.

§ Virginia Tech.

[1] Abbreviations: IDS, indigosulfonic acid, indigo disulfonate, indigo carmine; MOPS, 3-(*N*-morpholino)propanesulfonic acid; Tricine, *N*-[tris(hydroxymethyl)methyl]glycine; MES, 2-(4-morpholino)ethanesulfonic acid; P^N, wild-type MoFe protein P-cluster in the dithionite-reduced state; P^{1+}, P-cluster that is oxidized by one electron relative to the P^N state; P^{2+}, P-cluster that is oxidized by two electrons relative to the P^N state; P^{dt}, P-cluster of the β-188^{Cys} MoFe protein in the dithionite-reduced state; P^{red}, P-cluster of the β-188^{Cys} MoFe protein reduced relative to the P^{dt} state; P^{ox}, P-cluster of the β-188^{Cys} MoFe protein oxidized relative to the P^{dt} state; FeMo-cofactor, iron−molybdenum cofactor of nitrogenase; apo-MoFe protein, MoFe protein that does not contain FeMo-cofactor.

10.1021/bi982866b CCC: $18.00
Published on Web 04/16/1999

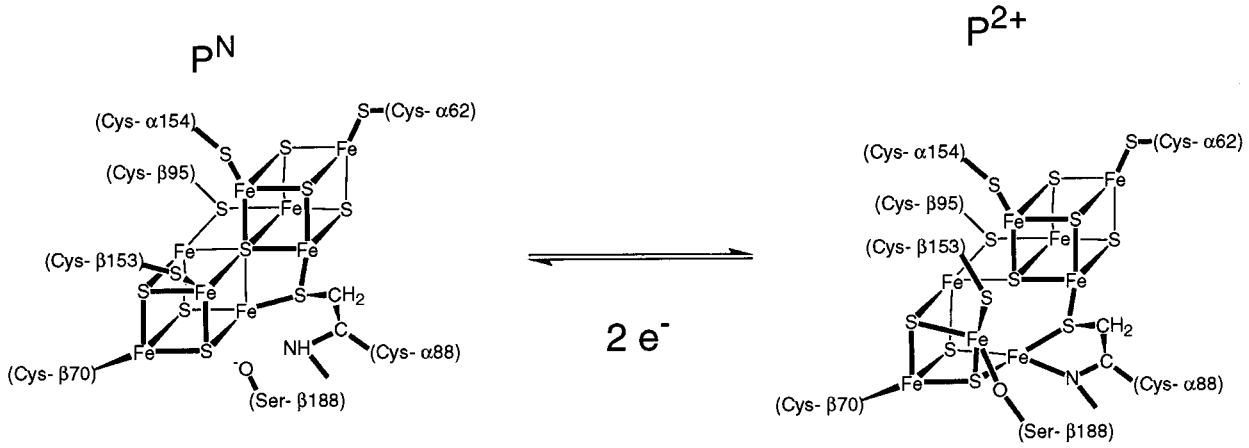

FIGURE 1: Models for the P^{2+} and P^N oxidation states of the P-cluster. Models for an oxidized (P^{ox}) or reduced (P^N) state of the P-cluster are based on the X-ray structures previously published (*13*). The P^{ox} state in (*13*) is assumed to be equivalent to the P^{2+} state.

Table 1: Activities of Wild-Type, β-188^{Cys}, and Apo-β-188^{Cys} MoFe Proteins

	specific activity [nmol of product·min^{-1}·(mg of MoFe protein)$^{-1}$][a]				
MoFe protein	C_2H_4 produced[b]	H_2 produced[c]	NH_3 produced[d]	MgATP hydrolysis[b]	ATP/e$^-$ [b]
wild-type	2200 ± 200	2900 ± 400	951 ± 93	8000 ± 1000	2.6 ± 0.4
β-188^{Cys}	630 ± 50	1100 ± 300	283 ± 2.5	6300 ± 1200	8.5 ± 1.6
apo-β-188^{Cys}	ND[e]	ND	−	2300 ± 300	N/A[f]

[a] Specific activities were determined with an Fe protein to MoFe protein molar ratio of 40:1. [b] Assays were performed under an atmosphere of 110 kPa Ar and 9 kPa C_2H_2. [c] Assays were performed under an atmosphere of 110 kPa Ar. [d] Assays were performed under an atmosphere of 110 kPa N_2. [e] ND, no activity detected. [f] N/A, not applicable.

stopped-flow and EPR spectroscopic results obtained during the reduction of dinitrogen were interpreted to indicate that the P-cluster becomes oxidized following a four-electron reduction of the MoFe protein (*8*).

Direct evidence for a redox role of the P-cluster during nitrogenase turnover remains elusive. One of the difficulties in understanding how the P-cluster functions during intercomponent electron transfer comes from the fact that all of the P-cluster Fe atoms present in the as-isolated, dithionite-reduced MoFe protein appear to be essentially in the ferrous oxidation state (*12*). Thus, it is difficult to envision how a resting state with P-clusters in this form, designated P^N, might accept additional electrons from the Fe protein. In addition, the P^N state of the P-cluster is diamagnetic, and so no EPR signature is available to monitor the P-cluster during turnover. In the present work, we have investigated the participation of the P-cluster in the nitrogenase catalytic mechanism by examining the properties of an altered MoFe protein for which a serine residue located near the P-cluster (β-subunit residue serine 188) was substituted by cysteine. This serine residue was chosen for substitution because it provides a reversible ligand to one of the Fe atoms of the P-cluster (*13*), being bound when the P-cluster is oxidized and not bound when the P-cluster is reduced with dithionite (Figure 1).

EXPERIMENTAL PROCEDURES

Strains and Protein Biochemistry. Site-directed mutagenesis, transformation (*14*), and gene-replacement methods (*15, 16*) were used to construct three *Azotobacter vinelandii* strains designated DJ995, DJ1190, and DJ1193. Strain DJ995 produces a MoFe protein that has seven histidine codons placed between *nifD* codons 481 and 482 (*17*), resulting in the addition of seven histidine residues onto the C-terminus of the MoFe protein α-subunit. Strains DJ1190 and DJ1193 were derived from and are isogenic with strain DJ995 except for the following mutations. Strain DJ1190 produces an altered MoFe protein with the β-subunit serine 188 residue substituted by cysteine. Strain DJ1193 was derived from strain DJ1190 and also has an insertion and deletion mutation within the *nifB* gene. Because the *nifB* gene product is required for FeMo-cofactor biosynthesis (*18*, *19*), strain DJ1193 produces an altered MoFe protein that does not contain FeMo-cofactor (apo-MoFe protein). MoFe proteins prepared from DJ995, DJ1190, and DJ1193 are respectively referred to as wild-type MoFe protein, β-188^{Cys} MoFe protein, and β-188^{Cys} apo-MoFe protein. MoFe proteins from strains DJ995, DJ1190, and DJ1193 were purified using a previously described Zn-based metal affinity chromatography procedure (*17*). Wild-type Fe protein and non-His-tagged MoFe protein were expressed and purified as previously described (*20*, *21*). The wild-type Fe and MoFe proteins had acetylene reduction specific activities of greater than 2000 nmol·min^{-1}·(mg of protein)$^{-1}$. In all of the following studies, the wild-type His-tagged and non-His-tagged MoFe proteins were compared and confirmed to behave the same (also see ref *17*).

Acetylene and proton reduction activities (*22*) and N_2 reduction activity (*23*) were determined using a 40:1 molar ratio of Fe protein to MoFe protein. MgATP hydrolysis rates were quantified using an HPLC-based method (*24*). Typical activities are given in Table 1. All protein manipulations were performed under anaerobic conditions maintained using either a Schlenk apparatus (*20*) or an argon-filled glovebox (Vacuum Atmospheres, Hawthorne, CA).

Redox Titrations. Potentiometric redox titrations were performed essentially as previously described (*24*). Protein samples were prepared for redox titrations by first passing

them over a Sephadex G-25 column equilibrated with buffer (50 mM Tricine, 50 mM MES containing 250 mM NaCl and adjusted to the designated pH with either HCl or NaOH). The redox mediators flavin mononucleotide ($E_m = -172$ and -238 mV), benzyl viologen ($E_m = -361$ mV), methyl viologen ($E_m = -440$ mV), and *N*,*N*′-propane-2,2′-dipyridinium ($E_m = -560$ mV) were used at final concentrations of 50 μM each. The redox potential of the titration solution was adjusted by the addition of small volumes of an oxidized 25 mM IDS solution, a 2 mM sodium dithionite solution, a 100 mM sodium dithionite solution, or a 10 mM solution of electrochemically reduced (*25*) *N*,*N*′-propane-2,2′-dipyridinium. At defined potentials, 200 μL samples were removed from the titration solution and were immediately frozen in calibrated quartz EPR tubes. The reference electrode was a Ag/AgCl microelectrode calibrated against a standard calomel electrode. Midpoint potentials have an estimated error of ± 10 mV and are reported relative to the normal hydrogen electrode (NHE). EPR signal intensities were measured from the peak-to-peak height for the $g = 1.97$ centered signal. Nonlinear, least-squares fits of the data to the Nernst equation were done using the computer program IgorPro (Wavemetrics, Lake Oswego, OR).

EPR Spectroscopy. EPR spectra were recorded on Bruker ESP300E spectrometers equipped with Oxford ESR 900 liquid helium cryostats. In all cases, 4 mm calibrated quartz EPR tubes (Wilmad, Buena, NJ) were used. High-field EPR spectra were recorded with a microwave frequency of 9.64 GHz, a modulation frequency of 100 kHz, a modulation amplitude of 12.6 G, a conversion time of 20.5 ms, and a time constant of 20.5 ms. The final spectra were the sum of 5 scans. Low-field EPR spectra were recorded with a microwave frequency of 9.5 GHz, a microwave power of 200 mW, a modulation frequency of 100 kHz, a modulation amplitude of 8 G, a conversion time of 40 ms, and a time constant of 160 ms. The final spectra were the sum of 6 scans.

For EPR analysis of proteins under turnover conditions, samples were prepared containing 100 μM MoFe protein, 50 μM Fe protein, 29 mM sodium dithionite, 10 mM MgATP, and a MgATP regenerating system (20 mM phosphocreatine, 0.3 mg/mL creatine phosphokinase, and 2 mg/mL bovine serum albumin) in 280 mM MOPS buffer, pH 7.0, under an atmosphere of 110 kPa Ar. Samples were incubated at 25 °C, and activity was initiated by the addition of MgATP. At the specified times, samples were removed from the reaction vial, transferred to quartz EPR tubes, and immediately frozen in liquid nitrogen.

EPR Signal Integration Methods. The intensities of EPR signals were quantified using the methods of Aasa and Vänngård (*26*), which allow integration of overlapping or incomplete EPR signals with $S \geq {}^1/_2$. The spin reference was the $g = 4.3$ EPR absorption peak arising from the dithionite-reduced, resting $S = {}^3/_2$ state of the FeMo-cofactor from wild-type MoFe protein (*27*). For EPR signals in the $g = 5-7$ region, the regions encompassing the absorbance peaks corresponding to the two $S = {}^5/_2$ manifolds were integrated individually and corrected for intensity and the missing *g*-values (*26*). Finally, the spectra were corrected for population utilizing a Boltzmann distribution (*28*, *29*) using *D* values published previously ($D = 5.1$ cm^{-1} for the $S = {}^3/_2$ signal of FeMo-cofactor (*30*) and $D = -3.2$ cm^{-1} for the P^{1+} state of the P-cluster (*29*)). Corrections were also applied to compensate for power and modulation amplitude differences between the sample and reference spectra (*31*). For the $S = {}^1/_2$ signal of the P-cluster, the total integrated intensity was also compared to a 0.3 mM Cu(EDTA) standard using standard methods (*31*).

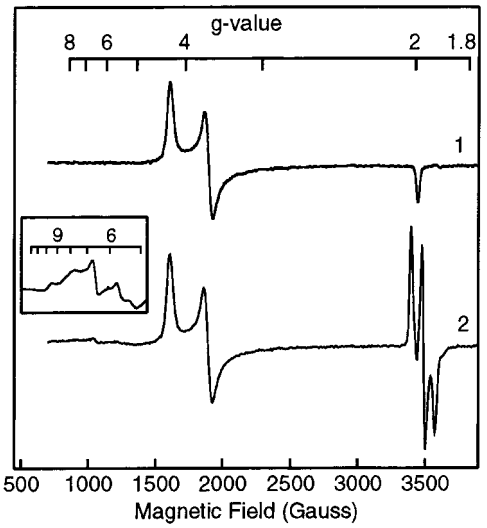

FIGURE 2: EPR spectra of the wild-type and β-188^{Cys} MoFe proteins in the dithionite-reduced state. Perpendicular mode EPR spectra are shown for the wild-type (trace 1) and β-188^{Cys} (trace 2 and inset) MoFe proteins. For traces 1 and 2, protein concentrations were 77 μM for the wild-type MoFe protein and 80 μM for the β-188^{Cys} MoFe protein, and the buffer was 100 mM MOPS, pH 7.0, with 250 mM NaCl and 2 mM dithionite. Spectra were recorded at 12 K with a microwave power of 2.01 mW. The concentration of β-188^{Cys} MoFe protein for the inset was 100 μM, and the buffer was 50 mM MES, pH 6.5, with 300 mM NaCl and 2 mM dithionite. The spectrum was recorded at 12 K with a microwave power of 200 mW.

RESULTS

Catalytic Activities. The catalytic properties of the purified β-188^{Cys} MoFe protein were determined in the presence of wild-type Fe protein, MgATP, a MgATP regenerating system, and the reductant dithionite. Under these conditions, the β-188^{Cys} MoFe protein was found to catalyze the reduction of acetylene, protons, or nitrogen at rates approximately 30% of that supported by the wild-type MoFe protein (Table 1). Under the appropriate assay conditions, the β-188^{Cys} MoFe protein retained approximately 80% of the wild-type nitrogenase MgATP hydrolysis activity. Thus, MgATP hydrolysis supported by the β-188^{Cys} MoFe protein was partially uncoupled from electron transfer when compared to the wild-type MoFe protein assayed under the same conditions (Table 1).

EPR of the β-188^{Cys} MoFe Protein. In the as-isolated, dithionite-reduced state, the wild-type MoFe protein exhibits a unique perpendicular mode EPR spectrum with *g*-values of 4.3, 3.7, and 2.0 (Figure 2, trace 1). This signal arises from the as-isolated, dithionite-reduced FeMo-cofactor, which is in a noninteger, $S = {}^3/_2$, spin state (*27*, *32*). In contrast, the P-cluster (P^N) is in an EPR-silent, $S = 0$, spin state. The EPR spectrum of the as-isolated, dithionite-reduced β-188^{Cys} MoFe protein at pH 7.0 is shown in Figure 2 (trace 2). A normal FeMo-cofactor signal is evident in the $g = 4$ region, confirming that the FeMo-cofactor environment has

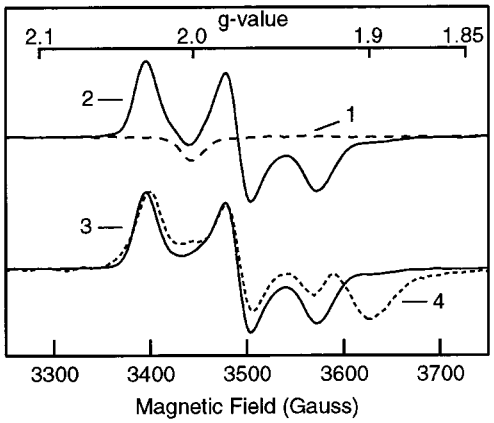

FIGURE 3: Comparison of EPR spectra for the wild-type MoFe protein, the β-188^{Cys} MoFe protein, and the apo-β-188^{Cys} MoFe protein. The $g = 2.0$ region of the perpendicular mode EPR spectrum is shown for the wild-type MoFe protein (trace 1), the β-188^{Cys} MoFe protein (trace 2), the β-188^{Cys} MoFe protein minus the wild-type MoFe protein (trace 3), and the apo-β-188^{Cys} MoFe protein (trace 4).

not been altered by the amino acid substitution. In addition, EPR signals were evident for the β-188^{Cys} MoFe protein at both high and low field. At high field, a new signal was centered at $g = 1.97$ ($g = 2.03, 1.97, 1.93$), corresponding to an $S = {}^1/_2$ spin state. Likewise, EPR signals were apparent at low field (Figure 2, inset). Examination of the temperature dependence suggests that all of the signals arise from excited state transitions with zero-field splitting (D) less than 0. Of these signals, inflections at $g = 7.7$ and $g = 6.7$ and 5.3 can be assigned to two $S = {}^5/_2$ spin state manifolds. These signals are very similar to signals which have been previously observed and are indicative of the P^{1+} oxidation state of the P-cluster (*29*). Another inflection at $g \sim 9.6$ was assigned to a very rhombic, $S = {}^5/_2$ spin system and is most likely due to a small amount of adventitious Fe present in the sample. Two other inflections at $g \sim 15.2$ and 5.7 were also observed; however, these signals have not been assigned. Integration of the $g_{av} = 1.97$ signal and the signals at $g \sim 7.7$ and 6.7 (see Experimental Procedures) indicates that these signals represent 0.6 spin/$\alpha\beta$-unit when compared to 1 spin/$\alpha\beta$-unit for FeMo-cofactor. The lower integration for the P-cluster probably represents a lower limit for the following reasons. First, quantification of these convoluted signals carries some uncertainty resulting in correction factors that must be applied to compensate for signal overlap, and the D values may be slightly different from the estimates used. Second, the full range of the two $S = {}^5/_2$ signals is not visible. Finally, there are some contributions from additional signals that could not be assigned, and therefore were not included in the integrations.

Given that the β-188^{Ser} residue is a ligand to the oxidized P-cluster in wild-type MoFe protein, the new EPR signals observed in the β-188^{Cys} MoFe protein were assigned to the P-cluster. To confirm this assignment, an apo-form of the β-188^{Cys} MoFe protein, which lacks FeMo-cofactor, was prepared and examined. The $g \sim 2$ region of the EPR spectrum for the β-188^{Cys} apo-MoFe protein is shown in Figure 3 (trace 4). The EPR spectrum for the β-188^{Cys} MoFe protein with the FeMo cofactor signal of the wild-type MoFe protein spectrum subtracted out is also shown (trace 3). The $g = 1.97$ centered EPR signal is retained in the apo-version

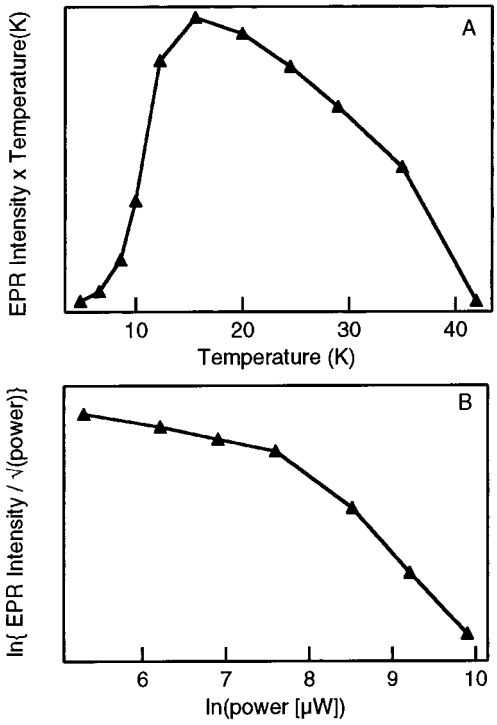

FIGURE 4: Temperature and power dependence of the intensity of the P-cluster signal of the β-188^{Cys} MoFe protein. Panel A: the temperature-weighted intensity of the $S = {}^1/_2$ P-cluster EPR signal for the β-188^{Cys} MoFe protein was plotted against the temperature. Spectra were recorded at a microwave power of 2.01 mW. Panel B: the natural logarithm of the signal intensity divided by the square root of the microwave power was plotted against the natural logarithm of the microwave power. Spectra were recorded at a temperature of 12 K. The β-188^{Cys} MoFe protein concentration was 84 μM, and the buffer was 100 mM MOPS, pH 7.0, with 250 mM NaCl and 2 mM dithionite.

of the β-188^{Cys} MoFe protein, confirming that the P-cluster is the source of the signal. Spectral subtraction of the β-188^{Cys} P-cluster EPR signal (trace 3) from the β-188^{Cys} apo-MoFe protein (trace 4) yields a spectrum similar to that previously assigned to damaged P-clusters present in the apo-MoFe protein from *Klebsiella pneumoniae* (*19*) and *A. vinelandii* (*17*).

The temperature and microwave power dependence of the β-188^{Cys} MoFe protein $g = 1.97$ centered EPR signal was determined as shown in Figure 4. This behavior is similar to that reported for the P^{1+} state of the P-cluster (*29*) and for [4Fe-4S] clusters in ferredoxins. All subsequent EPR studies were done at a temperature of 12 K and a microwave power of 2.0 mW. The P-cluster present in the as-isolated, dithionite-reduced form of the β-188^{Cys} MoFe protein is hereafter designated as P^{dt} in order to distinguish it from the P-cluster present in the wild-type MoFe protein prepared under the same conditions (P^N).

Redox Properties of the P-Cluster. The redox dependence of the $g = 1.97$ centered EPR signal for the β-188^{Cys} MoFe protein was examined by mediated voltammetry with detection by EPR. Figure 5 shows that upon changing the applied potential from -479 mV to -182 mV, the EPR signal disappears. The reversibility of this redox-dependent change in the EPR signal intensity was demonstrated by the return of the full intensity of the $g = 1.97$ centered EPR signal when the applied potential was returned back to -475 mV from -182 mV. It was also observed that the $g = 1.97$

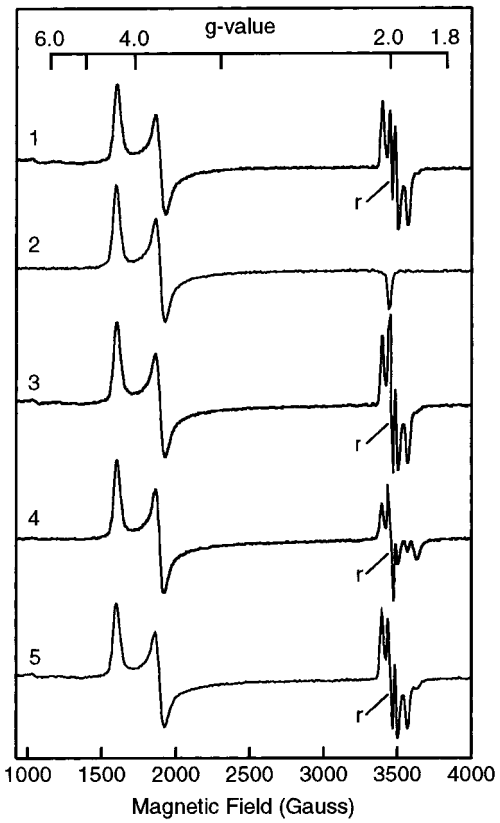

FIGURE 5: Dependence of the EPR signal intensity of the β-188^{Cys} MoFe protein on the reduction potential. Perpendicular mode EPR spectra were recorded for the β-188^{Cys} MoFe protein poised at different potentials in a mediated buffer solution as described under Experimental Procedures. In one sample, the applied potential started at −479 mV (trace 1) and was changed to −182 mV (trace 2). To confirm reversibility, an aliquot of the sample at −182 mV was returned to −475 mV (trace 3). In another sample, the applied potential was changed to −560 mV (trace 4). To confirm reversibility, an aliquot of the sample at −560 mV was returned to −473 mV (trace 5). Mediator radical EPR signals centered at $g = 2.0$ are marked with an "r". The β-188^{Cys} MoFe protein concentration was 75 μM.

centered EPR signal intensity decreased upon changing the solution potential to −560 mV. Again, this redox-dependent change in EPR signal intensity was reversible as evident by the return of the original signal intensity upon returning the applied potential to −473 mV. Thus, P^{dt} can be reversibly oxidized or reduced to yield states designated as P^{ox} or P^{red}, respectively. It is noted that a new EPR feature appears at $g = 1.89$ when the β-188^{Cys} MoFe protein is poised at −560 mV, indicating the possible presence of an EPR active species in the P^{red} state.

The dependence of the intensity of the $g = 1.97$ centered P-cluster EPR signal upon the applied potential is shown in Figure 6. An estimated midpoint potential (E_m) for the $P^{ox/dt}$ couple was calculated to be −390 mV at pH 8.0. The full EPR intensity for the P^{dt} state is probably not observable since a significant percentage of either the P^{ox} or the P^{red} state would also be present depending on the applied potential. Therefore, the E_m values presented are only estimates. The pH dependence of the apparent E_m value for the $P^{ox/dt}$ couple was examined by repeating the redox titration at pH 6.5. As can be seen, the lower pH shifted the apparent E_m for this couple to a more positive potential ($E_m = -290$ mV). The pH dependence for this couple is consistent with

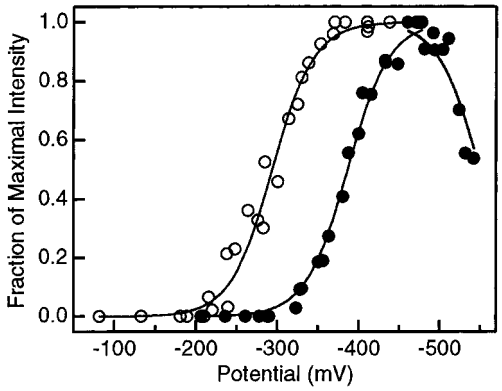

FIGURE 6: Redox titrations of the P-clusters of the β-188^{Cys} MoFe protein. Redox titrations were performed as outlined under Experimental Procedures for the $S = {}^1/_2$ signal of the β-188^{Cys} MoFe protein at pH 8.0 (●) and pH 6.5 (○). The peak-to-peak height of the P-cluster EPR signal was normalized to the maximum intensity observed. The solid lines represent nonlinear least-squares fits of the data to the Nernst equation where $n = 1$. The midpoint potentials were estimated to be −390 mV and −550 mV at pH 8.0, and −290 mV at pH 6.5. Potentials are relative to the normal hydrogen electrode (NHE).

a proton-coupled redox reaction, as was found for the wild-type MoFe protein $P^{2+/1+}$ redox couple (*33*). Because the β-188^{Cys} MoFe protein is unstable when poised at potentials below −550 mV, an E_m value could not be calculated for the $P^{dt/red}$ couple.

Turnover Studies. Earlier studies have shown that when wild-type MoFe protein is examined by EPR under substrate reducing conditions (with Fe protein, MgATP, a MgATP regenerating system, and the reductant dithionite), the intensity of the FeMo-cofactor signal decreases during turnover (*32*, *34*, *35*). If one of the reactants (e.g., MgATP) is consumed, and thus the nitrogenase substrate reduction reaction halts, the EPR signal arising from FeMo-cofactor returns to the initial resting intensity. These results have been interpreted as the conversion of a population of the resting state of FeMo-cofactor to an EPR-silent state during turnover, followed by relaxation back to the EPR-active, resting state upon termination of turnover (*32*, *34*, *35*). Because the β-188^{Cys} MoFe protein retained the ability to reduce substrates, and the P-cluster from the altered MoFe protein exhibited an EPR signature, it was possible to follow changes in the P-cluster during turnover using EPR. The intensities of the P-cluster signals for the β-188^{Cys} MoFe protein were observed to diminish during turnover (Figure 7). When MgATP was omitted from the mixture, or if MgADP was substituted for MgATP, no changes in the P-cluster EPR signals were observed, showing that the changes were dependent on MgATP. Upon exhaustion of the MgATP in the turnover sample (i.e., nonturnover conditions), the EPR signals arising from the P-cluster returned to the initial intensity, demonstrating reversibility of the observed changes and relaxation of the P-cluster back to the dithionite-reduced, resting state (P^{dt}).

DISCUSSION

Properties of the β-188^{Cys} MoFe Protein P-Cluster. In the wild-type MoFe protein, the P-cluster is known to exist in at least four different reversible oxidation states as shown in Scheme 1. In this scheme, P-clusters in the as-isolated, dithionite-reduced MoFe protein are designated P^N (*28*, *29*).

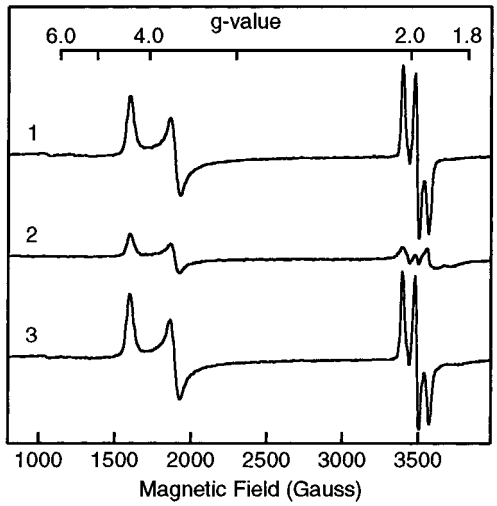

FIGURE 7: EPR spectra of the β-188^{Cys} MoFe protein under turnover conditions. EPR spectra were recorded for the β-188^{Cys} MoFe protein under proton reduction conditions as detailed under Experimental Procedures. Turnover was initiated by the addition of MgATP, and the reaction was quenched by freezing the sample in liquid nitrogen. EPR spectra are shown at 0 s (trace 1), 35 s (trace 2), and 27 min (trace 3) after initiation of the reaction.

Scheme 1

$$P^N \underset{}{\overset{E_{m1} = -309\ mV}{\rightleftharpoons}} P^{1+} \overset{E_{m2} = -309\ mV}{\rightleftharpoons} P^{2+} \overset{E_{m3} = +90\ mV}{\rightleftharpoons} P^{3+}$$

There is currently no evidence that P-clusters present in a catalytically active MoFe protein can be reduced further than P^N. The P^N state is diamagnetic and, therefore, EPR-silent. In contrast the P^{1+}, P^{2+}, and P^{3+} states are all paramagnetic, each giving rise to a characteristic EPR spectrum (*28*, *29*). Substitution of the β-188 serine residue by cysteine resulted in an altered MoFe protein that exhibits EPR signals in its as-isolated, dithionite-reduced state that arise from the P-cluster. The appearance of these EPR signals indicates that the electronic properties of P-clusters present in the altered MoFe protein must be different from those in wild-type MoFe protein. Changing β-188^{Ser} of the MoFe protein to a glycine (*33*) did not result in the EPR signals reported here, indicating that these signals must arise from the presence of the cysteine at this position.

Consideration of the redox and spectroscopic properties of the P-clusters in the wild-type and β-188^{Cys} MoFe proteins, and the changes that would be predicted from the substitution of a redox-dependent serine ligand for a cysteine ligand allows a model to be developed to explain the observations presented here, and to gain insights into the properties and function of the P-cluster. Several observations suggest that the dithionite-reduced, resting state (P^{dt}) of the P-cluster in the β-188^{Cys} MoFe protein is comparable to the one electron oxidized (P^{1+}) state of the P-cluster in the wild-type MoFe protein. First, the similarity between g values for the $S = {}^5/_2$ EPR signals of the P^{dt} and P^{1+} states suggests a similar core oxidation state. Second, the fact that both the P^{1+} and P^{dt} states are mixed spin states, with $S = {}^5/_2$, ${}^1/_2$, points to the similarity. Third, consideration of the midpoint potentials for the various couples further suggests a similarity. The midpoint potentials for each of the P-cluster couples in wild-type MoFe protein at pH 8.0 are shown in Scheme 1 (28). It was recently shown that the midpoint potential for the $P^{2+/1+}$ couple (E_{m2}) for the wild-type MoFe protein is pH dependent (−53 mV/pH unit) (*33*). The apparent E_m for the $P^{ox/dt}$ couple of the β-188^{Cys} MoFe protein is also observed to be pH dependent. This suggests that the $P^{2+/1+}$ and $P^{ox/dt}$ couples of the wild-type and β-188^{Cys} MoFe proteins are similar. This could be explained by a shift in the E_m values for each of the P-cluster couples in the β-188^{Cys} MoFe protein to more negative values. In fact, the estimated midpoint potentials for the P-cluster couples of the β-188^{Cys} MoFe protein are significantly more negative than those of the wild-type MoFe protein. The $P^{ox/dt}$ couple has an estimated E_m of −390 mV at pH 8.0, which is 80 mV more negative than the lowest E_m value reported for the P-cluster from the wild-type MoFe protein at the same pH value. Similarly, based on the data shown in Figure 6, the E_m for the $P^{dt/red}$ couple is more negative than the lowest potentials observed for P-cluster couples from the wild-type MoFe protein. Thus, the placement of a cysteine residue at position β-188 shifts the E_m values for the P-cluster couples to more negative values, with the comparable states probably being P^{red} and P^N, P^{dt} and P^{1+}, and P^{ox} and P^{2+} for the β-188^{Cys} and wild-type MoFe proteins, respectively.

How could the presence of a cysteine residue at position 188 shift the E_m values for the P-cluster couples to more negative potentials? Previous studies involving ligand exchanges for [Fe-S] clusters in other proteins have shown that replacing a cysteine ligand with a serine ligand often results in negative shifts in the E_m value (*36*−*39*). The observation from the present work that changing a serine ligand to a cysteine ligand results in negative shifts in the E_m values for the P-cluster couples is therefore different from the effect observed in other [Fe-S] clusters. This can be explained by the unique redox-dependent structural changes that occur in the P-cluster compared to the other cases. It is known that upon oxidation of the wild-type MoFe protein from the P^N state to the P^{2+} state, the serine at the β-188 position becomes a ligand to one of the Fe atoms of the P-cluster (*13*). If an analogous redox-dependent ligand exchange occurred in the β-188^{Cys} version of the P-cluster, then the cysteine residue would become a ligand to the same Fe atom upon oxidation. Since the cysteine thiol is expected to favor being bound to the Fe compared to the serine alkoxide (*40*, *41*), the presence of the cysteine should favor the oxidized state, altering the redox equilibrium toward the oxidized state. This would result in a shift of the E_m value for this couple to a more negative potential. This is consistent with the large negative shifts in the E_m values measured for the β-188^{Cys} MoFe protein.

Redox Role of the P-Cluster during Turnover. The presence of EPR signals arising from the P-clusters in the β-188^{Cys} MoFe protein provides an opportunity to monitor redox changes in the P-cluster during nitrogenase turnover conditions. It was found that the EPR signal intensity greatly diminished when the β-188^{Cys} MoFe protein was incubated under turnover conditions, which included reduced Fe protein and MgATP. It is reasonable to conclude from this observation that the Fe protein transfers an electron to the P-cluster in the presence of MgATP. The absolute requirement of MgATP for this reaction was confirmed in control experiments in which MgADP was added in place of MgATP, and no changes in the intensity of the P-cluster EPR signals were observed. The reduction of an oxidized state of the P-cluster (P^{2+}) in the wild-type MoFe protein was previously observed

to occur readily when reduced Fe protein and MgATP were added. The FeMo-cofactor $S = {}^3/_2$ EPR signal in wild-type MoFe protein diminishes in intensity during turnover conditions, indicating reduction by the Fe protein when MgATP is present. Thus, the present work provides direct spectroscopic evidence that the P-clusters undergo redox changes during nitrogenase turnover in the β-188^{Cys} MoFe protein. Considering the location of the P-clusters between the Fe protein [4Fe-4S] cluster and FeMo-cofactor as observed in the X-ray structures of nitrogenase complexes (*10*, *11*), the current findings support a model in which the P-clusters function as intermediate electron-transfer sites during the delivery of electrons ultimately to substrates.

ACKNOWLEDGMENT

We thank Drs. Brian Hales and Morton Sorlie for their assistance in EPR spin quantification and Drs. Mike Johnson and Jennifer Huyett for valuable suggestions.

REFERENCES

1. Dean, D. R., Bolin, J. T., and Zheng, L. (1993) *J. Bacteriol. 175*, 6737−6744.
2. Kim, J., and Rees, D. C. (1992) *Science 257*, 1677−1682.
3. Burgess, B. K. (1990) *Chem. Rev. 90*, 1377−1406.
4. Georgiadis, M. M., Komiya, H., Chakrabarti, P., Woo, D., Kornuc, J. J., and Rees, D. C. (1992) *Science 257*, 1653−1659.
5. Hageman, R. V., and Burris, R. H. (1978) *Proc. Natl. Acad. Sci. U.S.A. 75*, 2699−2702.
6. Ma, L., Brosius, M. A., and Burgess, B. K. (1996) *J. Biol. Chem. 271*, 10528−10532.
7. Peters, J. W., Fisher, K., Newton, W. E., and Dean, D. R. (1995) *J. Biol. Chem. 270*, 27007−27013.
8. Lowe, D. J., Fisher, K., and Thorneley, R. N. F. (1993) *Biochem. J. 292*, 93−98.
9. Angove, H. C., Yoo, S. J., Munck, E., and Burgess, B. K. (1998) *J. Biol. Chem. 273*, 26330−26337.
10. Schindelin, H., Kisker, C., Schlessman, J. L., Howard, J. B., and Rees, D. C. (1997) *Nature 387*, 370−376.
11. Rees, D. C., Schindelin, H., Kisker, C., Schlessman, J., Peters, J. W., Seefeldt, L. C., and Howard, J. B. (1998) in *Biological Nitrogen Fixation for the 21st Century* (Elmerich, C., Kondorosi, A., and Newton, W. E., Eds.), pp 11−16, Kluwer Academic Publishers, Boston.
12. Surerus, K. K., Hendrich, M. P., Christie, P. D., Rottgardt, D., Orme-Johnson, W. H., and Münck, E. (1992) *J. Am. Chem. Soc. 114*, 8579−8590.
13. Peters, J. W., Stowell, M. H. B., Soltis, S. M., Finnegan, M. G., Johnson, M. K., and Rees, D. C. (1997) *Biochemistry 36*, 1181−1187.
14. Page, W. J., and Von Tigerstrom, M. (1979) *J. Bacteriol. 139*, 1058−1061.
15. Jacobson, M. R., Cash, V. L., Weiss, M. C., Laird, N. F., Newton, W. E., and Dean, D. R. (1989) *Mol. Gen. Genet. 219*, 49−57.
16. Robinson, A. C., Burgess, B. K., and Dean, D. R. (1986) *J. Bacteriol. 166*, 180−186.
17. Christiansen, J., Goodwin, P. J., Lanzilotta, W. N., Seefeldt, L. C., and Dean, D. R. (1998) *Biochemistry 37*, 12611−12623.
18. Paustian, T. D., Shah, V. K., and Roberts, G. P. (1990) *Biochemistry 29*, 3515−3522.
19. Hawkes, T. R., and Smith, B. E. (1983) *Biochem. J. 209*, 43−50.
20. Burgess, B. K., Jacobs, D. B., and Stiefel, E. I. (1980) *Biochim. Biophys. Acta 614*, 196−209.
21. Seefeldt, L. C., and Mortenson, L. E. (1993) *Protein Sci. 2*, 93−102.
22. Seefeldt, L. C., and Ensign, S. A. (1994) *Anal. Biochem. 221*, 379−386.
23. Chaney, A. L., and Marbach, E. P. (1962) *Clin. Chem. 8*, 130−132.
24. Ryle, M. J., Lanzilotta, W. N., Mortenson, L. E., Watt, G. D., and Seefeldt, L. C. (1995) *J. Biol. Chem. 270*, 13112−13117.
25. Lanzilotta, W. N., and Seefeldt, L. C. (1997) *Biochemistry 36*, 12976−12983.
26. Aasa, R., and Vänngård, T. (1975) *J. Magn. Reson. 19*, 308−315.
27. Rawlings, J., Shah, V. K., Chisnell, J. R., Brill, W. J., Zimmerman, R., Munck, E., and Orme-Johnson, W. H. (1978) *J. Biol. Chem. 253*, 1001−1004.
28. Pierik, A. J., Wassink, H., Haaker, H., and Hagen, W. R. (1993) *Eur. J. Biochem. 212*, 51−61.
29. Tittsworth, R. C., and Hales, B. J. (1993) *J. Am. Chem. Soc. 115*, 9763−9767.
30. Münck, E., Rhodes, H., Orme-Johnson, W. H., Davis, L. C., Brill, W. J., and Shah, V. K. (1975) *Biochim. Biophys. Acta 400*, 32−53.
31. Fee, J. A. (1978) *Methods Enzymol. 49*, 512−528.
32. Orme-Johnson, W. H., Hamilton, W. D., Jones, T. L., Tso, M. Y. W., Burris, R. H., Shah, V. K., and Brill, W. J. (1972) *Proc. Natl. Acad. Sci. U.S.A. 69*, 3142−3145.
33. Lanzilotta, W. N., Christiansen, J., Dean, D. R., and Seefeldt, L. C. (1998) *Biochemistry 37*, 11376−11384.
34. Mortenson, L. E., Zumft, W. G., and Palmer, G. (1973) *Biochim. Biophys. Acta 292*, 422−435.
35. Smith, B. E., Lowe, D. J., and Bray, R. C. (1972) *Biochem. J. 130*, 641−643.
36. Meyer, J., Gaillard, J., and Lutz, M. (1995) *Biochem. Biophys. Res. Commun. 212*, 827−833.
37. Werth, M. T., Cecchini, G., Manodori, A., Ackrell, B. A. C., Schroder, I., Gunsalus, R. P., and Johnson, M. K. (1990) *Proc. Natl. Acad. Sci. U.S.A. 87*, 8965−8969.
38. Xiao, Z., Lavery, M. J., Ayhan, M., Scrofani, S. D. B., Wilce, M. C. J., Guss, J. M., Tregloan, P. A., George, G. N., and Wedd, A. G. (1998) *J. Am. Chem. Soc. 120*, 4135−4150.
39. Babini, E., Bertini, I., Borsari, M., Capozzi, F., Dikiy, A., Eltis, L. D., and Luchinat, C. (1996) *J. Am. Chem. Soc. 118*, 75−80.
40. Cheng, H., Xia, B., Reed, G. H., and Markely, J. L. (1994) *Biochemistry 33*, 3155−3164.
41. Xia, B., Cheng, H., Bandarian, V., Reed, G. H., and Markley, J. L. (1996) *Biochemistry 35*, 9488−9495.

BI982866B